hepatoma cell lines. 11th International Meeting on Hepatitis C Virus and Related Viruses, 2004 年 10 月.

15) Sakamoto, S., Shiroki, K., Suzuki, R., Matsuura, Y., Suzuki, T., and Miyamura, T. HCV capsid assembly: role of basic residue clusters in the core protein. 11th International Meeting on Hepatitis C Virus and Related Viruses, 2004 年 10 月.

16) Moriishi, K., Mochizuki, R., Abe, T., Mori, Y., Moriya, K., Koike, K., Suzuki, T., Miyamura, T., and Matsuura, Y. PA28gamma-dependent degradation of HCV core protein in the nucleus in vivo. 11th International Meeting on Hepatitis C Virus and Related Viruses, 2004 年 10 月.

17) Murakami, K., Ishii, K., Yoshizaki, S., Aizaki, H., Tanaka, K., Shoji, I., Sata, T., Suzuki, T., Bartenshlarger, R., and Miyamura, T. Assembly of HCV-like particles in three-dimensional cultures. 11th International Meeting on Hepatitis C Virus and Related Viruses, 2004 年 10 月.

18) 松浦善治、森屋恭爾、小池和彦、田中啓二、鈴木哲朗、宮村達男、森石恆司. HCV コア蛋白質の成熟および分解の分子機構. 第 63 回日本癌学会学術総会, 2004 年 9 月.

19) Suzuki, T. Assembly of HCV-like particles in the three-dimensional cultures of human hepatoma cells. Fuji Forum 2004. 2004 年 8 月.

20) 森屋恭爾、田島 藍、堤 武也、伊藤晃成、三好秀征、藤江 肇、新谷良澄、下池貴志、鈴木哲朗、宮村達男、堀江利治、小池和彦. HCV core 蛋白質はミトコンドリア電子伝達系 complex I 機能を障害する. 第 40 回日本肝臓学会総会, 2004 年 6 月.

G. 知的所有権の取得状況

なし

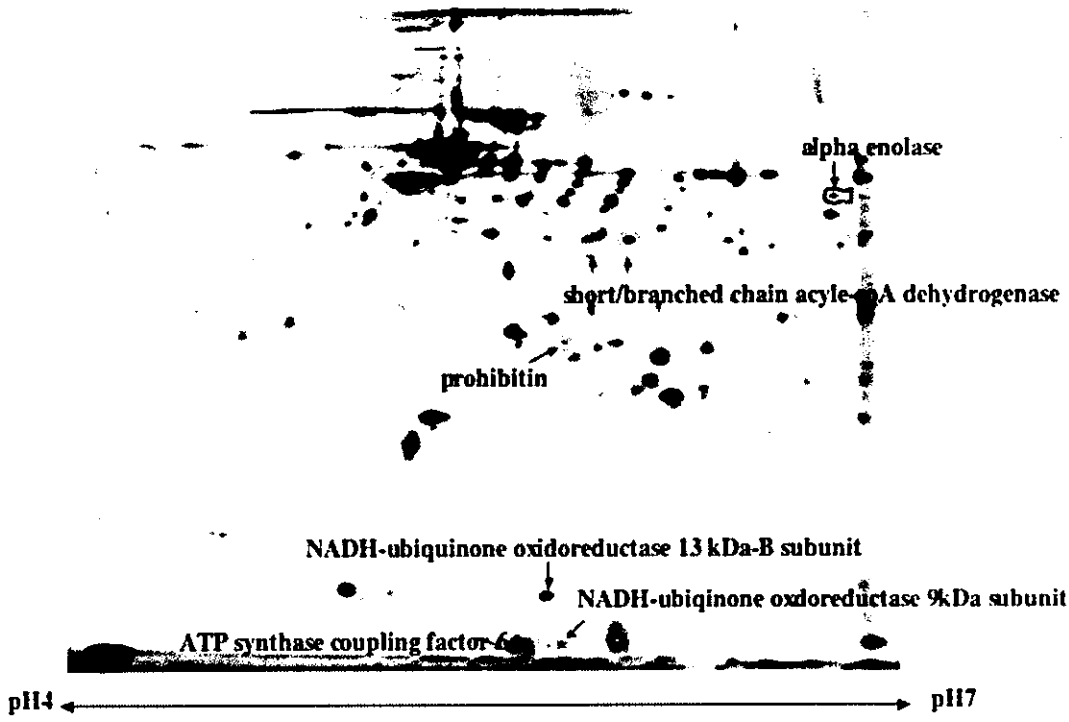

図１．Hepswx細胞ミトコンドリア画分の二次元電気泳動

	Spot NO.	Protein name	Av.Ratio (394/SWX)	T-test
Hep394<SWX	452	short/branched chain acyle-coA dehydrogenase	-2.32	0.00018
	449	short/branched chain acyle-coA dehydrogenase	-2.31	0.00055
	340	alpha enolase	-2.27	0.056
Hep394>SWX	602	prohibitin	1.93	0.023
Hep394=SWX	780	NADH-ubiquinone oxidoreductase 13 kDa-B subunit	1.07	
	798	NADH-ubiqinone oxdoreductase 9kDa subunit	1.17	
	802	ATP synthase coupling factor 6	1.03	

表１．全HCV蛋白産生細胞（Hep394)のミトコンドリアで発現が有意に変動した蛋白

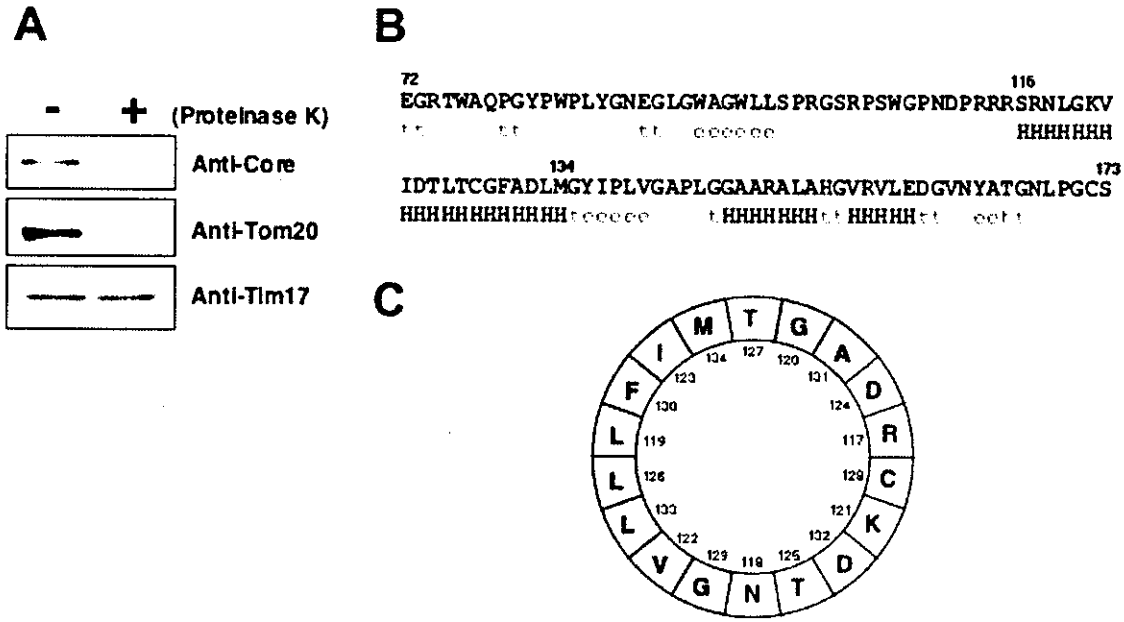

図２．(A)Protease protection assay. (B)推定される二次構造. (C)α-Helical plot.

厚生労働科学研究費補助金（肝炎等克服緊急対策研究事業）
トランスジェニック・マウスを用いた肝発がんメカニズムの解析
分担研究報告書

肝炎・肝細胞癌における酸化ストレスの関与

分担研究者　塚本 和久　東京大学医学部付属病院糖尿病・代謝内科　助手

研究要旨：発癌・ウイルス肝炎など、さまざまな疾患において酸化ストレスが重要な役割を果たすことが提唱されている。一昨年・昨年の研究において、過酸化リン脂質を水解して酸化ストレスを減弱する酵素であるPAF-AHが、発癌・ウイルス肝炎と同様に酸化ストレスが大きく関与すると考えられる動脈硬化や糸球体腎炎に対して良好な効果を有することを見出すと同時に、糸球体腎炎に対する効果を検討した実験において、アデノウイルスによる肝障害がラットにおいてPAF-AH (PAF acetylhydrolase)により抑制されることを明らかにした。本年度は、マウスにおいて、PAF-AH過剰発現がアデノウイルスによる肝障害に対してどのような効果を及ぼすのか、また、その結果を踏まえ、四塩化炭素およびN-ニトロソジメチルアミン(N-NDMA)による肝障害に対して、PAF-AHあるいはPAF-AHと同様に酸化ストレス抑制効果があると考えられているHO-1がどのような効果を有するのか、を検討した。まず、正常マウスにおいては、PAF-AH過剰発現はアデノウイルス投与による肝障害を、ラットにおける検討の場合と同様に、有意に抑制した。しかし、四塩化炭素およびN-NDMAによる肝障害モデルにPAF-AHあるいはHO-1を発現させても、今回検討した用量ではその生存率には大きな効果を有さなかった。現在、投与四塩化炭素およびN-NDMA投与量を変更して更なる検討を行っているところである。

A．研究目的

発癌、炎症、動脈硬化症、腎疾患など、様々な疾患において酸化ストレスは重要な役割を果たすことが提唱されている。

スーパーオキサイドをはじめ、酸化ストレスを引き起こす物質は各種存在するが、その中でも過酸化脂質は強力なメディエーターであることが知られている。PAF-AH (PAF acetylhydrolase)は、元来炎症のメディエーターであるPAFを水解して不活化する酵素として発見された酵素である。近年、PAF-AHは過酸化脂質をも水解して生物学的に活性のある過酸化脂質を不活化することが明らかとなってきており、SOD (super-oxide dismutase)などと並んで酸化ストレス改善に重要であることが唱えられている。我々は、一昨年および昨年の研究により、

PAF-AHが、発癌・ウイルス肝炎と同様に酸化ストレスが大きく関与すると考えられる動脈硬化や糸球体腎炎に対して良好な効果を有することを見出すと同時に、糸球体腎炎に対する効果を検討した実験においてアデノウイルスによる肝障害がラットにおいてPAF-AHにより抑制されることを明らかにした。本年度は、PAF-AHが、マウスにおいてもアデノウイルスによる肝障害を抑制するのか、を検討するとともに、酸化ストレスがその肝障害に役割を演ずると考えられている四塩化炭素およびN-NDMA投与による肝障害モデル動物に及ぼすPAF-AHの効果を検討した。

B．研究方法

I. アデノウイルスによる肝障害に対する効果

8週齢の野生型マウス（C57BL6/J）に、PAF-AHをコードするアデノウイルスベクター（AdPAFAH）あるいはコントロールアデノウイルスベクター(AdLacZ: b-galactosidaseをコードするベクター)、およびPBSを尾静脈より投与（$3X10^9$ pfu/個体）し、投与前、投与後3日目、7日目、14日目、21日目の血漿を採取してトランスアミナーゼの経時的変化を検討した。

II. 四塩化炭素による肝障害に対する効果

8週齢のC57BL6/JマウスにAdPAFAH、AdLacZ、あるいはAdHO1(ヘムオキシゲナーゼ1をコードするアデノウイルスベクター)を尾静脈より投与（$4X10^9$ pfu/個体）した後、翌日より四塩化炭素を連日10日間、以降の3週間は2回/週で、一回あたり0.6ml/kg BWで腹腔内投与した(総投与量9.6 ml/kg BW)。投与の際には、四塩化炭素はオリーブ油で1：2に希釈した。各群8頭を用いた。これらのマウスの生存率を観察した。

III. N-NDMAによる肝障害に対する効果

8週齢のC57BL6/JマウスにAdPAFAH、AdLacZ（$3X10^9$ pfu/個体）、あるいはPBSを尾静脈より投与し、その翌日にPBSにて500倍希釈したN-ニトロソジメチルアミン(N-NDMA)を1頭あたり300ml腹腔内投与した。各アデノウイルス投与群は4頭、PBS群には3頭を用いた。N-NDMA投与後の生存率を観察した。

C．研究結果

I. アデノウイルスによる肝障害に対する効果

ウイルス投与後のGPT値の経過を図1に示す。図に示したとおり、PAFAHウイルスを投与したマウスにおいて、ウイルス投与後にPBS群と比較してGPTの有意な上昇は見られるものの、LacZウイルスを投与した群と比較して、有意にその肝障害は軽減されていた。

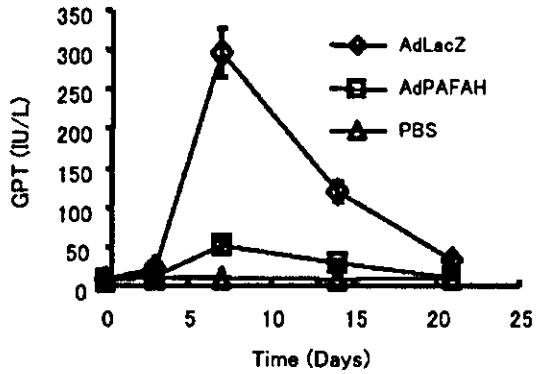

図1．C57BL6/JマウスにAdPAFAH (n=11)、AdLacZ (n=11)およびPBS (n=10)を投与後のGPTの経過。データは、平均値±SEMで示す。

II. 四塩化炭素投与による肝障害に対する

効果

PAF-AH および HO-1 過剰発現の効果を図２に示す。図に示すように、四塩化炭素惹起性の肝不全死亡率に対して、PAF-AH あるいは HO-1 による保護効果は認めることはできなかった。

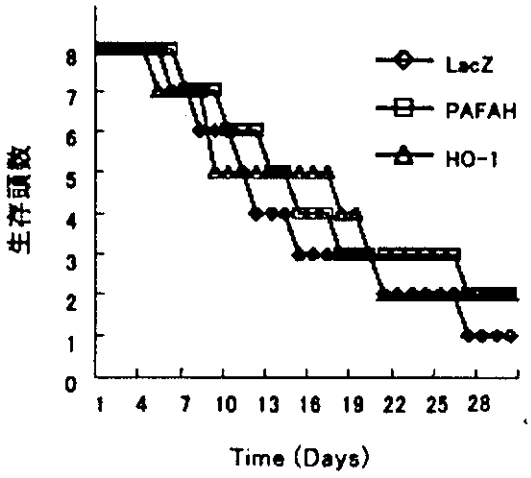

図２．各種アデノウイルスを投与後、翌日より四塩化炭素をプロトコールに従い（詳細は研究方法参照）腹腔内投与し、その後の生存率を検討した。Kaplan-Myer 法にての検討で、有意差は認められなかった。

III. N-NDMA による肝障害に対する効果

PBS 投与群 (n=3)、AdLacZ 投与群 (n=4)とも、N-NDMA 投与後３日目までに、すべて死亡した。AdPAF　AH 群 (n=4)においては、３頭が N-NDMA 投与後３日目までに死亡したが、１頭のみ 10 日目まで生存した。このマウスにおいては、N-NDMA 投与後に著明な肥満が認められた。

D．考察

酸化ストレスは、肝炎、発癌など、炎症が関与する様々な疾患において重要な役割を担う。今年度の研究は、昨年度・一昨年度の PAF-AH の生理学的機能解明およびアデノウイルスによるラット肝障害に対する効果の検討を発展させて、マウスを用いた各種肝炎・肝障害に対する効果の検討を行った。

結果に示したとおり、PAF-AH はマウスにおいてもアデノウイルスによる肝障害を軽減する作用を有していた。しかし、その肝障害に酸化ストレスが関与すると考えられている四塩化炭素および N-NDMA を投与した実験においては、今回の検討量ではその保護作用を証明することはできなかった。

四塩化炭素および N-NDMA において、PAF-AH あるいは HO-1 の肝保護作用を明白に証明できなかった原因として、今回用いた試薬の投与量がマウスにとっては大量であったと考えられる。今回の用量設定は、以前に報告されている論文を参照したが、今一度、特に N-NDMA に関しては、用量設定を行う必要性がある。また、四塩化炭素における実験においては、現在我々が使用しているアデノウイルスは第二世代のアデノウイルスであり、第一世代アデノウイルスよりも transgene の発現期間が長期ではあるものの、やはりその発現は投与後２週間経過すると非常に低下する、という欠点を持っているも確かである。現在、N-NDMA による肝障害がより軽度である投与量設定を開始しているとともに、長期間の transgene 発現が可能なアデノウイルスベクターの開発を進めているところである。

なお、N-NDMA で比較的長期間生存したマウスにおいて、著明な肥満が認められた点に関しても、今後さらに頭数を増やすことにより、その原因究明を行いたいと考えている。

E．結論

PAF-AH は、ラットのみならずマウスにおいてもアデノウイルスによる肝障害を抑制した。しかし、今回用いたプロトコ

ールによる四塩化炭素および N-NDMA による、肝不全死からマウスを保護する効果は認めなかった。今後、薬剤投与量を調節することにより、PAFAH が酸化ストレスによる肝障害を軽減させる作用を有するかどうかの検討をさらに進める予定である。

F．健康危険情報

なし。

G．研究発表

1．論文発表

1.Shintani Y. Fujie H. Miyoshi H. Tsutsumi T. Tsukamoto K. Kimura S. Moriya K. Koike K. Hepatitis C Virus Infection and Diabetes : Direct Involvement of the Virus in the Development of Insulin Resistance. *Gastroenterology* 126:840-848, 2004

2.Iso-O N. Noto H. Hara M. Togo M. Karasawa K. Ohashi N. Noiri E. Hashimoto Y. Kadowaki T. Kimura S. Watanabe T. Tsukamoto K. Adenovirus-mediated gene transfer and lipoprotein-mediated protein delivery of plasma PAF-AH ameliorates proteinuria in rat model of glomerulosclerosis. *Molecular Therapy* (in press)

2．学会発表

1. 磯尾直之，能登洋，唐沢健，佐藤博亮，東郷眞子，原眞純，橋本佳明，木村哲，塚本和久、門脇孝　PAF-アセチルヒドロラーゼ（PAF-AH）は抗酸化作用により腎糸球体硬化症の進展を抑制する　第36回日本動脈硬化学会総会　２００４年７月，福岡

H．知的所有権の出願・登録状況

1．特許取得

なし。

2．実用新案登録

なし。

3．その他

なし。

厚生労働科学研究費補助金（肝炎等克服緊急対策研究事業）
トランスジェニック･マウスを用いた肝発がんメカニズムの解析
分担研究報告書

モデルを用いたＣ型肝炎治療法の開発

分担研究者　森屋 恭爾　東京大学感染制御部　講師

研究要旨　我々はHCV 感染により脂肪肝ならびに脂質代謝異常、糖代謝異常が引き起こされることをマウスモデルで示してきた。又、HIV 感染に対する抗ウイルス剤治療の際、重篤な脂肪肝が引き起こされ治療が中断されることが見られる。この２つの病態はミトコンドリア障害が一つの因子になっていることが推定されている。また、C 型肝炎の治療においては、HCV を排除することが感染症であるＣ型慢性肝炎を治療する上で最上であることに疑いはないが、リバビリン併用ペグ・インターフェロン治療が主体となった現在においても、なお、４０～５０％の患者ではHCV 排除は不可能である。従って、ウイルス排除不能の場合にも、肝病態を感染させる方策の追求が必要であると言える。今回我々は、ミトコンドリア保護作用をもつ FK506（タクロリムス）をHCV コア遺伝子導入トランスジェニックマウスに投与し、脂質代謝および糖代謝等病態が改善されることを確認した。抗免疫作用を有しない FK506 のanalog を投与することにより、肝脂肪化、インスリン抵抗性といったＣ型肝炎の悪化促進因子の改善が望め、HCV 病態進行抑制が期待できる。

A. 研究目的

抗ウイルス剤によるHCV 治療は進歩をとげているが、副作用による重篤な脂肪肝により治療中断を選択しなければならない症例も多い。又、Ｃ型肝炎では肝臓にsteatosis（脂肪化）が出現することが肝線維化の増悪因子であることから、肝臓の脂肪化を抑止する薬剤のスクリーニングをHCV コア遺伝子導入トランスジェニックマウスを用いて行う。

B. 研究方法

３ヶ月齢のHCV コア遺伝子導入トランスジェニックマウス♂に対し、FK506（0.1mg/kg）ならびにPlacebo 投与を筋肉注射週３回、同様に非トランスジェニックマウス兄弟マウスについても３ヶ月齢♂に対しFK506（0.1mg/kg）あるいはPlacebo 投与を行った後、肝臓の脂質量、構成脂肪酸量、血糖値、インスリン値を検討した。

C. 研究結果

HCV コア遺伝子導入トランスジェニックマウスに認められた①肝臓の脂肪量の増加、②構成脂肪酸に占める C16:1、C18:1 などの不飽和脂肪酸の増加、③インスリン抵抗性のいずれもが FK506 投与により非トランスジェニックマウス兄弟マウスの Placebo 群と同様のレベルまで改善した。
非トランスジェニックマウス兄弟マウス群では FK506 においてもインスリン分泌が低下していた。

D. 考察

HCV コア蛋白による肝臓の脂肪化にはミトコンドリア障害が関与していることが強く示唆されている。FK506 は、免疫抑制剤として広く臨床への応用が行われているが、核カルシニューリンへの作用とともにミトコンドリア機能保護作用をもつというデータがある。今回の我々の結果から FK506 の有するミトコンドリア保護作用によって HCV コア蛋白による肝臓の脂質代謝異常が改善していることが初めて証明された。又、FK506 は、HCV コア蛋白の有無にかかわらずインスリン分泌低下能を有している事が示された。

E. 結論

ミトコンドリア保護作用を持つ FK506 によって、肝臓の脂肪化が抑制されることが示された。免疫抑制作用を有しない FK506 の誘導体物質によって、抗ウイルス作用を直接持たない薬剤での C 型肝炎の肝病態改善が抑制可能であることが示された。

F. 健康危険情報

なし。

G. 研究発表

1) Miyoshi H, Fujie H, Moriya K, Shintani Y, Tsutsumi T, Makuuchi M, Kimura S, Koike K. Methylation status of suppressor of cytokine signaling-1 gene in hepatocellular carcinoma. J Gastroenterol 39:563-569, 2004.
2) Shintani Y, Fujie H, Miyoshi H, Tsutsumi T, Kimura S, Moriya K, Koike K. Hepatitis C virus and diabetes: direct involvement of the virus in the development of insulin resistance. Gastroenterology 126:840-848, 2004.
3) Koike K, Fujie H, Shintani Y, Miyoshi H, Moriya K. Hepatitis C and Diabetes Mellitus: what is the metabolic pathway? Gastroenterology 127:1280-1281, 2004.
4) Koike K. Hepatitis C as a metabolic disease: HCV induces insulin resistance. Intervirology 2005 in press.
5) Miyoshi H, Fujie H, Shintani Y, Tsutsumi T, Shinzawa S, Makuuchi M, Kokudo N, Matsuura Y, Suzuki T, Miyamura T, Moriya K, Koike K. Hepatitis C Virus Core

Protein Exerts an Inhibitory Effect on Suppressor of Cytokine Signaling (SOCS)-1 Gene Expression. J Hepatol 2005 in press.
6) Koike K. Hepatitis C as a metabolic disease: implication for the pathogenesis of NASH. Hepatol Res 2005 in press.
7) Koike K, Moriya K. Metabolic aspects of hepatitis C: steatohepatitis distinct from NASH. J Gastroenterol 2005 in press.
8) Hatakeyama S, Moriya K, Saijo M, Morisawa Y, Kurane I, Koike K, Kimura S, Morikawa S. Persisting humoral anti-smallpox immunity among current Japanese population after the discontinuation in 1976 of routine smallpox vaccinations. Clin Diagn Lab Immun 2005 in press.

研究成果の刊行に関する一覧

1) Miyoshi H, Fujie H, Moriya K, Shintani Y, Tsutsumi T, Makuuchi M, Kimura S, Koike K. Methylation status of suppressor of cytokine signaling-1 gene in hepatocellular carcinoma. J Gastroenterol 39:563-569, 2004.

2) Shintani Y, Fujie H, Miyoshi H, Tsutsumi T, Kimura S, Moriya K, Koike K. Hepatitis C virus and diabetes: direct involvement of the virus in the development of insulin resistance. Gastroenterology 126:840-848, 2004.

3) Koike K, Fujie H, Shintani Y, Miyoshi H, Moriya K. Hepatitis C and Diabetes Mellitus: what is the metabolic pathway? Gastroenterology 127:1280-1281, 2004.

4) Koike K. Hepatitis C as a metabolic disease: HCV induces insulin resistance. Intervirology 2005 in press.

5) Miyoshi H, Fujie H, Shintani Y, Tsutsumi T, Shinzawa S, Makuuchi M, Kokudo N, Matsuura Y, Suzuki T, Miyamura T, Moriya K, Koike K. Hepatitis C Virus Core Protein Exerts an Inhibitory Effect on Suppressor of Cytokine Signaling (SOCS)-1 Gene Expression. J Hepatol 2005 in press.

6) Koike K. Hepatitis C as a metabolic disease: implication for the pathogenesis of NASH. Hepatol Res 2005 in press.

7) Koike K, Moriya K. Metabolic aspects of hepatitis C: steatohepatitis distinct from NASH. J Gastroenterol 2005 in press.

8) Hatakeyama S, Moriya K, Saijo M, Morisawa Y, Kurane I, Koike K, Kimura S, Morikawa S. Persisting humoral anti-smallpox immunity among current Japanese population after the discontinuation in 1976 of routine smallpox vaccinations. Clin Diagn Lab Immun 2005 in press.

9) Masubuchi Y, Suda C, Horie T. Involvement of mitochondrial permeability transition in acetaminophen-induced liver injury in mice. J. Hepatol. 42 (1), 110-116, 2005.

10) Iso-O N. Noto H. Hara M. Togo M. Karasawa K. Ohashi N. Noiri E.

Hashimoto Y. Kadowaki T. Kimura S. Watanabe T. Tsukamoto K. Adenovirus-mediated gene transfer and lipoprotein-mediated protein delivery of plasma PAF-AH ameliorates proteinuria in rat model of glomerulosclerosis. *Molecular Therapy* (in press)

11) Ishikawa T., Fukushima Y., Shiobara Y., Kishimoto T., Tanno S., Shoji I., Suzuki T., Matsui T., Shimada Y., Ohyama T., Nagai R., and Miyamura T. An outbreak of hepatitis C virus infection in an outpatient clinic. J. Gastroemterol. Hepatol., (2005) (in press).

12) Suzuki, T., and Suzuki, R. Maturation and assembly of hepatitis C virus core protein. *In*: FLAVIVIRIDAE: Pathogenesis, Molecular Biology and genetics. (2005) (in press).

13) Suzuki R., Sakamoto S., Tsutsumi T., Rikimaru A., Shimoike T., Mizumoto K., Matsuura Y., Miyamura T., and Suzuki T. Molecular determinants for subcellular localization of hepatitis C virus core protein. J. Virol., 79: 1271-1281 (2005).

14) Suzuki T., Suzuki R., Li J., Hijikata M., Matsuda M., Li T-C., Matsuura Y., Mishiro S., and Miyamura T. Identification of basal promoter and enhancer elements in an untranslated region of the TT virus genome. J. Virol., 78: 10820-10824 (2004).

15) 小池和彦. B型肝炎 内科外来診療実践ガイド MP 21:150-160, 2004.

16) 小池和彦. 性感染症診断・治療ガイドライン B型肝炎 日本性感染症学会雑誌 15:52-54, 2004.

17) 三好秀征、小池和彦. C型肝炎ウイルス感染と酸化ストレスについて 肝臓 45：285-294, 2004.

18) 小池和彦. HIV・HCV 重複感染時の診療ガイドラインについて. 日本病院薬剤師会雑誌 40:941-944, 2004.

19) 小池和彦、三好秀征. C型肝炎ウイルスと他のウイルスの重複感染症感染とその病態的意義. 臨床とウイルス 32：163-169,2004.

20) 小池和彦. HCV コア蛋白トランスジェニックマウスによる肝発癌機構の解明. ウイルス性肝炎（上） 日本臨床 62：131-134,2004.

21) 森屋恭爾、小池和彦. C型肝炎感染はどうして高率に慢性化するのか（ウイルス因子とホスト因子）. ウイルス性肝炎（上） 日本臨床 62：405-407,2004.
22) 小池和彦. A型肝炎. 感染症 竹田美文、木村哲編集. 朝倉書店2004、p98-99.
23) 小池和彦. E型肝炎. 感染症 竹田美文、木村哲編集. 朝倉書店2004、p100-102.
24) 小池和彦. 急性ウイルス肝炎（A型とE型を除く）. 感染症 竹田美文、木村哲編集. 朝倉書店2004、p198-201.
25) 森屋恭爾、小池和彦. 肝炎ウイルス感染の予防. Medicina 41:1687-1689,2004.
26) 小池和彦. C型慢性肝炎. ドクターサロン 48：817-820,2004.
27) 宮村達男、河岡義裕、小池和彦. 感染症新時代. 現代医療 36：2154-2173,2004.
28) 塚田訓久、小池和彦. HIV・HCV重複感染症の現状. 現代医療 36：2294-2298,2004.
29) 鈴木哲朗 C型肝炎ウイルスと肝発癌 臨床とウイルス 32: 156-162 (2004).
30) 村上恭子、鈴木哲朗. HCVの新たな感染系及びHCV-RNA複製系の開発動向. ウイルス性肝炎（上）日本臨床 増刊号, 62: 111-115 (2004).
31) 相崎英樹、鈴木哲朗. HCV-RNA複製およびHCV増殖の分子メカニズム. ウイルス性肝炎（上）日本臨床 増刊号, 62: 81-84 (2004).
32) 鈴木哲朗、松浦善治. HCV感染レセプター. 肝疾患Review 2004. 117-120 (2004).

JOURNAL OF VIROLOGY, Jan. 2005, p. 1271–1281
0022-538X/05/$08.00+0 doi:10.1128/JVI.79.2.1271–1281.2005

Vol. 79, No. 2

Molecular Determinants for Subcellular Localization of Hepatitis C Virus Core Protein

Ryosuke Suzuki,[1] Shinichiro Sakamoto,[1] Takeya Tsutsumi,[1] Akiko Rikimaru,[1,2] Keiko Tanaka,[3] Takashi Shimoike,[1] Kohji Moriishi,[4] Takuya Iwasaki,[3,5] Kiyohisa Mizumoto,[2] Yoshiharu Matsuura,[4] Tatsuo Miyamura,[1] and Tetsuro Suzuki[1]*

Department of Virology II, National Institute of Infectious Diseases, Shinjuku-ku,[1] Department of Biochemistry, School of Pharmaceutical Sciences, Kitasato University, Minato-ku,[2] and Department of Pathology, National Institute of Infectious Diseases, Shinjuku-ku,[3] Tokyo, Research Center for Emerging Infectious Diseases, Research Institute for Microbial Diseases, Osaka University, Suita-shi, Osaka,[4] and Department of Pathology, Institute of Tropical Medicine, Nagasaki University, Nagasaki-shi, Nagasaki,[5] Japan

Received 21 June 2004/Accepted 26 July 2004

Hepatitis C virus (HCV) core protein is a putative nucleocapsid protein with a number of regulatory functions. In tissue culture cells, HCV core protein is mainly located at the endoplasmic reticulum as well as mitochondria and lipid droplets within the cytoplasm. However, it is also detected in the nucleus in some cells. To elucidate the mechanisms by which cellular trafficking of the protein is controlled, we performed subcellular fractionation experiments and used confocal microscopy to examine the distribution of heterologously expressed fusion proteins involving various deletions and point mutations of the HCV core combined with green fluorescent proteins. We demonstrated that a region spanning amino acids 112 to 152 can mediate association of the core protein not only with the ER but also with the mitochondrial outer membrane. This region contains an 18-amino-acid motif which is predicted to form an amphipathic α-helix structure. With regard to the nuclear targeting of the core protein, we identified a novel bipartite nuclear localization signal, which requires two out of three basic-residue clusters for efficient nuclear translocation, possibly by occupying binding sites on importin-α. Differences in the cellular trafficking of HCV core protein, achieved and maintained by multiple targeting functions as mentioned above, may in part regulate the diverse range of biological roles of the core protein.

Hepatitis C virus (HCV), the most important causative agent of posttransfusion and sporadic non-A, non-B hepatitis, is a positive-stranded RNA virus belonging to the family *Flaviviridae* (7). A precursor polyprotein of about 3,000 amino acids is encoded by a large open reading frame of the genome and undergoes cellular and viral protease-mediated posttranslational modification to produce a series of structural and nonstructural proteins (8, 13, 16).

HCV core protein, which is derived from the N terminus of the viral polyprotein, forms multimers and interacts physically with the viral RNA to constitute the nucleocapsid (28, 47, 50). Tissue transglutaminase is responsible for stabilizing the core protein by cross-linking it into a dimeric form (26). In addition, the core viral protein has properties which enable it to modulate a number of cellular processes, including transcription, inhibition or stimulation of apoptosis, and suppression of host immunity, as reviewed previously (21, 29, 51, 52). Several studies suggest that expression of the core protein affects mitochondrial function and lipid metabolism. The core protein increases the cellular production of reactive oxygen species with subsequent increases in lipid peroxidation (35, 39). The viral protein also colocalizes with human apolipoprotein AII, associates with lipid droplets, and has the capacity to influence metabolic events involving lipid storage (2, 17, 30, 36, 44). In addition, the core protein reduces microsomal triglyceride transfer, leading to defects in very low density lipoprotein assembly and secretion (40). Furthermore, the HCV core protein has transforming potential in some cells under certain conditions (5, 42). Transgenic mice expressing this protein in the liver develop hepatic steatosis due to increased oxidative stress in the absence of inflammation, with subsequent development of hepatocellular carcinoma (34, 36). These results suggest that the HCV core protein might play a pivotal role in the pathogenesis of hepatitis C in addition to its role as a structural component of the viral capsid.

The amino acid sequence of the core protein is well conserved among different HCV isolates and genotypes compared to other HCV proteins. The N-terminal domain of the HCV core protein is highly basic, while its C terminus is hydrophobic. Although several core proteins of various sizes exist (17 to 23 kDa) (15, 23, 25, 49, 56), two processing events result in the predominant production of a 21-kDa core protein. Both of these events utilize the endoplasmic reticulum (ER). The first one is to be cleaved from downstream envelope protein E1 at position 191, where the C-terminal hydrophobic domain serves as a putative signal peptide sequence. Subsequently, the signal sequence of 13 or 18 residues is processed by signal peptide peptidase (19, 23, 56).

The HCV core protein is found primarily within the membranes of cytoplasmic organelles, but it is also found in the nucleus (23, 48, 56). Immunofluorescence studies show a punc-

* Corresponding author. Mailing address: Department of Virology II, National Institute of Infectious Diseases, 1-23-1 Toyama, Shinjuku-ku, Tokyo, Japan 162-8640. Phone: (81) 3-5285-1111. Fax: (81) 3-5285-1161. E-mail: tesuzuki@nih.go.jp.

tate pattern, consistent with ER localization, as well as perinuclear localization (15, 24, 32, 46, 56). Some studies suggest direct effects of the core protein on mitochondrial function. In fact, the core protein localizes to the mitochondria (34, 39). The N-terminal domain of the core protein contains three stretches of arginine- and lysine-rich sequences. Translocation of the core protein to the nucleus, mediated by these basic-residue stretches which function as nuclear localization signals (NLSs), is observed (6, 48). In addition, Moriishi et al. demonstrated that the N-terminal region of the core protein is also essential for nuclear retention through its interaction with the proteasome activator PA28γ (33).

In this study, we found a region that is important for localization of the mature core protein to the ER and to the mitochondrial outer membrane. We also identified a novel bipartite NLS responsible for nuclear targeting of the core protein, presumably via an importin-dependent pathway.

MATERIALS AND METHODS

Plasmid construction. The construction of a plasmid expressing the full-length core protein of 191 amino acids, pCAGC191, was described previously (49). pGFP, a construct expressing green fluorescent protein (GFP) with a C-terminal Myc epitope tag sequences, was prepared as follows. pCMV/Myc/mito/GFP (Invitrogen Corp., Carlsbad, Calif.) was digested with PmlI, followed by treatment with the Klenow fragment of DNA polymerase I. The resultant linear fragment was ligated to a PstI linker (GCTGCAGC) and digested with PstI to remove the mitochondrial targeting signal sequence, followed by self-ligation. A series of HCV core-GFP fusion constructs were made by amplifying the core gene fragments with PCR with primers containing Flag epitope tag sequences (sense) and a PstI site (both). After digestion with PstI, the segments were inserted into the PstI site of pGFP. A series of GFP-core-E1 fusion constructs were made by amplifying core and E1 gene fragments with PCR with primers containing a NotI site. After digestion with NotI, the segments were inserted into the NotI site of pGFP.

pGEX-4T-1 (Amersham Bioscience Corp., Piscataway, N.J.) was used to express core protein fused with glutathione *S*-transferase (GST) in *Escherichia coli*. Core cDNA fragments encoding amino acids 1 to 71 were inserted into the EcoRI site of pGEX-4T-1. Alanine substitutions were introduced into the core protein by PCR mutagenesis with primers containing base alterations. The PCR products were then cloned into pCR2.1 (Invitrogen Corp.) and verified by DNA sequencing. Individual cDNAs were excised and inserted separately into pGFP or pGEX-4T-1. The primer sequences used in this study are available from the authors upon request.

Plasmid pRSET-hSRP1α (54), containing importin-α cDNA under the control of a T7 promoter, was kindly provided by Karsten Weis (University of California, Berkeley). A cDNA clone of importin-α possessing 14 residues (MYPYDVP DYGGGGS), derived in part from the hemagglutinin (HA) tag at the N terminus, was constructed by PCR. The resultant linear fragment was inserted under the control of a CAG promoter of pCAGGS and designated pCAG-HA-imp.

Cell culture and transfection. Human embryonic kidney 293T cells were maintained in Dulbecco's modified Eagle's medium supplemented with 100 units of penicillin per ml, 100 μg of streptomycin per ml, and 10% fetal bovine serum at 37°C in a 5% CO_2 incubator. Monolayers of 293T cells were transfected with plasmid DNA in the presence of Lipofectamine (Gibco-BRL, Life Technologies, Gaithersburg, Md.) according to the manufacturer's instructions.

Confocal immunofluorescence microscopy. Transfected cells were grown on glass coverslips. Two days after transfection, cells were fixed with 4% paraformaldehyde in phosphate-buffered saline (PBS) for 20 min at room temperature. Intracellular localization of HCV core-GFP fusion proteins was visualized in cells transfected with a variety of GFP fusion constructs.

In order to detect the HCV core protein by immunofluorescence, fixed cells were permeabilized with 0.2% Triton X-100 in PBS for 3 min at room temperature, followed by blocking with a nonfat milk solution (Block Ace; Snow Brand Milk Products Co., Sapporo, Japan). The cells were then incubated with anticore monoclonal antibody B2 (Anogen, Mississauga, Canada) for 60 min at room temperature, followed by incubation with fluorescein isothiocyanate-conjugated rabbit anti-mouse immunoglobulin G (IgG) (ICN Pharmaceuticals, Aurora, Ohio) for 45 min. To visualize mitochondria, MitoTracker Red CM-H_2XRos (Molecular Probes, Eugene, Oreg.) was added to the culture medium to a final concentration of 100 nM and incubated for 120 min at 37°C prior to fixation. To visualize the ER, goat anticalregulin antibody (Santa Cruz Biotechnology, Santa Cruz, Calif.) and rhodamine-conjugated rabbit anti-goat IgG (ICN Pharmaceuticals) were used as the first and second antibodies, respectively. To visualize HA-importin-α, mouse anti-HA antibody (Roche Molecular Biochemicals, Indianapolis, Ind.) and rhodamine-conjugated goat anti-mouse IgG (ICN Pharmaceuticals) were used as the first and second antibodies, respectively. All specimens were examined with an LSM510 laser scanning confocal microscope (Carl Zeiss, Oberkochen, Germany).

Immunoelectron microscopy. Cells were transfected as described above. After 2 days, cells were fixed with 3% paraformaldehyde and 0.1% glutaraldehyde in 0.1 M PBS (pH 7.4). Free aldehyde groups were quenched with 50 mM NH_4Cl in PBS. The cell pellets were embedded at progressively lower temperatures (down to −35°C) in Lowicryl k4M according to an established protocol (43). Ultrathin sections were prepared and mounted on carbon-coated nickel grids. To perform electron microscopy, Lowicryl k4M ultrathin sections, mounted on grids, were floated on a droplet of PBS containing 1% bovine serum albumin, 0.1% Triton X-100, and 0.1% Tween 20 for 10 min, after which they were exposed to droplets of mouse anticore monoclonal antibody (Anogen) diluted in PBS for 45 min. Following this, they were rinsed twice for 5 min each in PBS and incubated with anti-mouse IgG-coated 10-nm immunogold particles (British Biocell, Cardiff, United Kingdom) for 45 min. After rinsing with PBS and distilled water, the grids and embedded sections were air dried and exposed to uranyl and lead acetate contrast agents.

Subcellular fractionation. All steps were performed at 4°C in the presence of a protease inhibitor cocktail called Complete (Roche Molecular Biochemicals). To isolate the ER fraction, transfected cells were washed with PBS, lysed in homogenization buffer A (50 mM Tris-HCl [pH 8.0], 1 mM β-mercaptoethanol, 1 mM EDTA, and 0.32 M sucrose), and then centrifuged at 5,000 × *g* for 10 min. The supernatant was then collected and centrifuged at 105,000 × *g* for 1 h. The pellet was disrupted in lysis buffer (50 mM Tris-HCl [pH 7.5], 150 mM NaCl, 1% NP-40, 1 mM dithiothreitol, 1 mM sodium orthovanadate, and 10 mM sodium fluoride), after which it was centrifuged at 15,000 × *g* for 20 min. The resulting supernatant was used as the ER fraction.

To isolate the mitochondrial fraction, transfected cells were washed with PBS and homogenized in ice-cold homogenization buffer B (200 mM mannitol, 50 mM sucrose, 1 mM EDTA, and 10 mM Tris-HCl) at pH 7.4. The supernatant was then centrifuged at 1,000 × *g* for 10 min to remove large debris and nuclei. The resulting supernatant was then centrifuged at 20,000 × *g* for 20 min to obtain crude mitochondria. The crude mitochondria pellet was subfractionated in Nycodenz gradients for further purification of mitochondria. Nycodenz (Axis-Shield PoC AS, Oslo, Norway) solution at 50% (wt/vol) was prepared in buffer containing 5 mM Tris-HCl and 1 mM EDTA at pH 7.4. This stock solution was then diluted with buffer containing 0.25 M sucrose, 5 mM Tris-HCl, and 1 mM EDTA at pH 7.4 before use. The crude mitochondrial pellets was suspended in 4 ml of 25% Nycodenz solution and overlaid onto the following discontinuous Nycodenz gradients: 1 ml of 40%, 1 ml of 34%, and 2 ml of 30%. The samples were topped off with 2 ml of 23% Nycodenz solution after placement onto the discontinuous gradients. The tubes were then centrifuged at 52,000 × *g* for 90 min. The dense band seen after centrifugation at the 25 to 30% interface was recovered as the purified mitochondrial fraction.

To determine the submitochondrial localization pattern of the core protein, mitochondria were resuspended in SH buffer (0.6 M sorbitol and 20 mM HEPES-KOH [pH 7.2]) in the absence or presence of 30 μg of proteinase K per ml after purification by Nycodenz density gradient centrifugation. Samples were incubated for 30 min at 0°C, after which protease digestion was halted by the addition of *p*-aminophenyl methanesulfonyl fluoride hydrochloride (*p*-APMSF) (5 mM). Proteins lysed in sodium dodecyl sulfate (SDS) sample buffer were analyzed by SDS-polyacrylamide gel electrophoresis (PAGE) and immunoblotted as described below.

Immunoblot analysis. The proteins were transferred to a polyvinylidene difluoride membrane (Immobilon; Millipore, Tokyo, Japan) after separation by SDS-PAGE. After blocking, the membranes were probed with monoclonal- or polyclonal-antibody against core protein (Anogen), prohibitin (Neo Markers, Fremont, Calif.), ribophorin I (Santa Cruz Biotechnology), translocase of the outer membrane (Tom) 20 (Santa Cruz Biotechnology), translocase of the inner membrane (Tim) 17 (Santa Cruz Biotechnology), or GFP (Santa Cruz Biotechnology). Immunoblots were developed as previously described (15).

GST pulldown assay. *Escherichia coli* BL21 cells were transformed with GST-core fusion plasmids and grown at 37°C. Expression of the fusion protein was induced by 1 mM isopropyl-β-D-thiogalactopyranoside at 37°C for 3 h. Bacteria were harvested, suspended in lysis buffer (1% Triton X-100 in PBS), and soni-

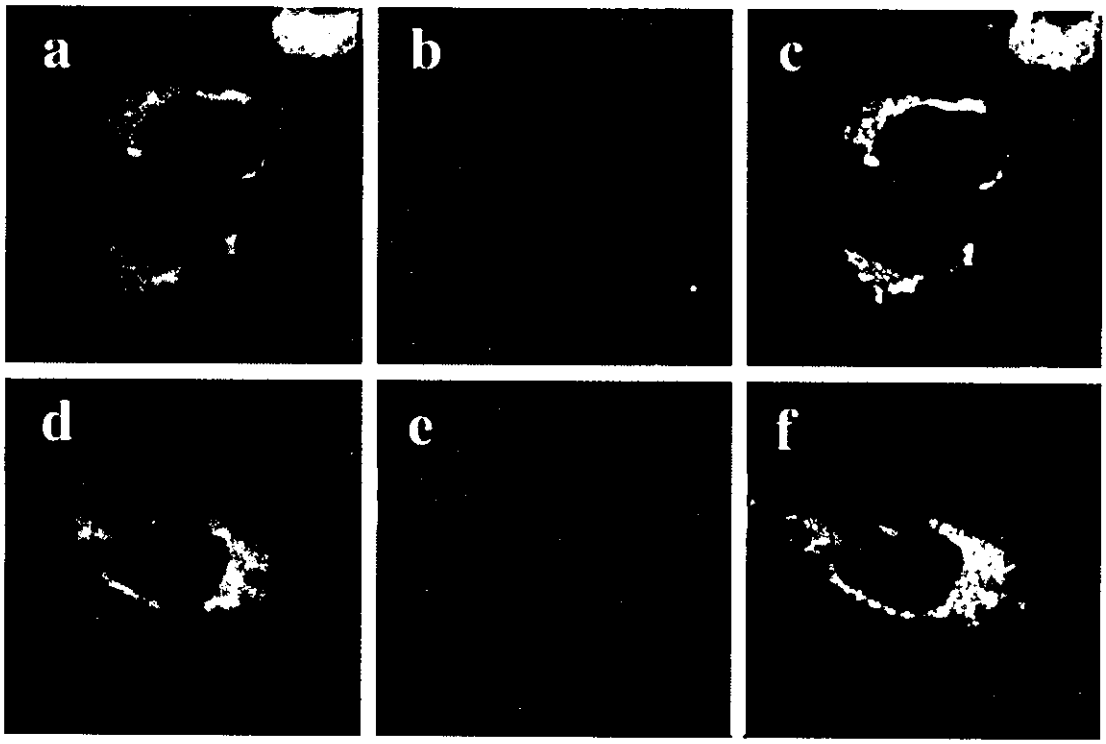

FIG. 1. Confocal analysis of double staining for HCV core protein and ER or mitochondria. 293T cells transfected with full-length HCV core expression plasmid, pCAGC191 were allowed to express the plasmid for 2 days. Transfected cells were fixed directly (a to c) or fixed after loading with Mitotracker (d to f). After permeabilization with Triton X-100, cells were subjected to immunofluorescence staining with a mouse anticore antibody. A goat anticalregulin antibody was used for ER staining. The green signals corresponding to the core were found with a fluorescein isothiocyanate-conjugated rabbit anti-mouse IgG (a and d). The red signals corresponding to the ER were obtained with a rhodamine-conjugated rabbit anti-goat IgG secondary antibody (b). Mitochondria were stained with the mitochondrion-selective dye Mitotracker (e). Overlay resulted in yellow signals indicative of colocalization (c and f).

cated on ice. GST and GST fusion proteins were purified from bacterial lysates with glutathione-Sepharose beads (Amersham Bioscience Corp.). The beads were washed four times with lysis buffer. Approximately equal amounts of purified protein, as estimated by Coomassie brilliant blue staining, were used for the binding assays. For pulldown assays, in vitro transcription and translation of importin-α was done with pRSET-hSRP1α and the TNT-coupled reticulocyte lysate system (Promega Corp., Madison, Wis.) with T7 RNA polymerase. The reaction was carried out at 30°C for 4 h in the presence of [^{35}S]methionine/cysteine (ICN Pharmaceuticals). The translation product was then incubated with glutathione-Sepharose beads bound to GST fusion proteins in 1 ml of binding buffer (40 mM HEPES [pH 7.5], 100 mM KCl, 0.1% NP-40, and 20 mM 2-mercaptoethanol) at 4°C for 1 h. The beads were washed four times with binding buffer, and the pulldown complexes were separated by SDS-PAGE on 15% polyacrylamide gels. The gels were then fixed, dried, and analyzed with autoradiography.

RESULTS

Subcellular localization of HCV core protein. To assess the subcellular localization of HCV core protein, we first analyzed cells transfected with a full-length core-expressing construct by confocal microscopy. In accordance with previous observations (2, 15, 32, 45, 56), a granular cytoplasmic staining pattern of the core protein was observed in 293T (Fig. 1) and human hepatoblastoma HepG2 (data not shown) cells. Dual staining of transfected cells with antibody against the ER protein calregulin along with anticore antibody confirmed the ER localization of the core protein (Fig. 1a, b, and c show the core,

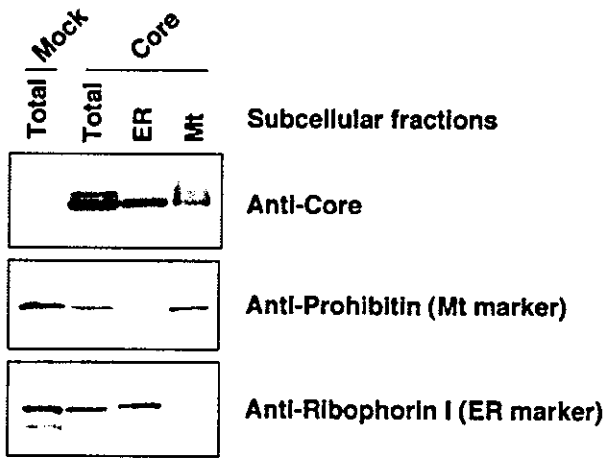

FIG. 2. Subcellular distribution of HCV core protein analyzed by immunoblotting. ER and mitochondrial (Mt) fractions were isolated from 293T cells expressing the full-length core protein (Core) or nontransfected cells (Mock) 2 days after transfection. Equal amounts of protein from each fraction as well as whole cell lysates (Total) were subjected to immunoblotting with a monoclonal antibody against either HCV core, prohibitin, or ribophorin I.

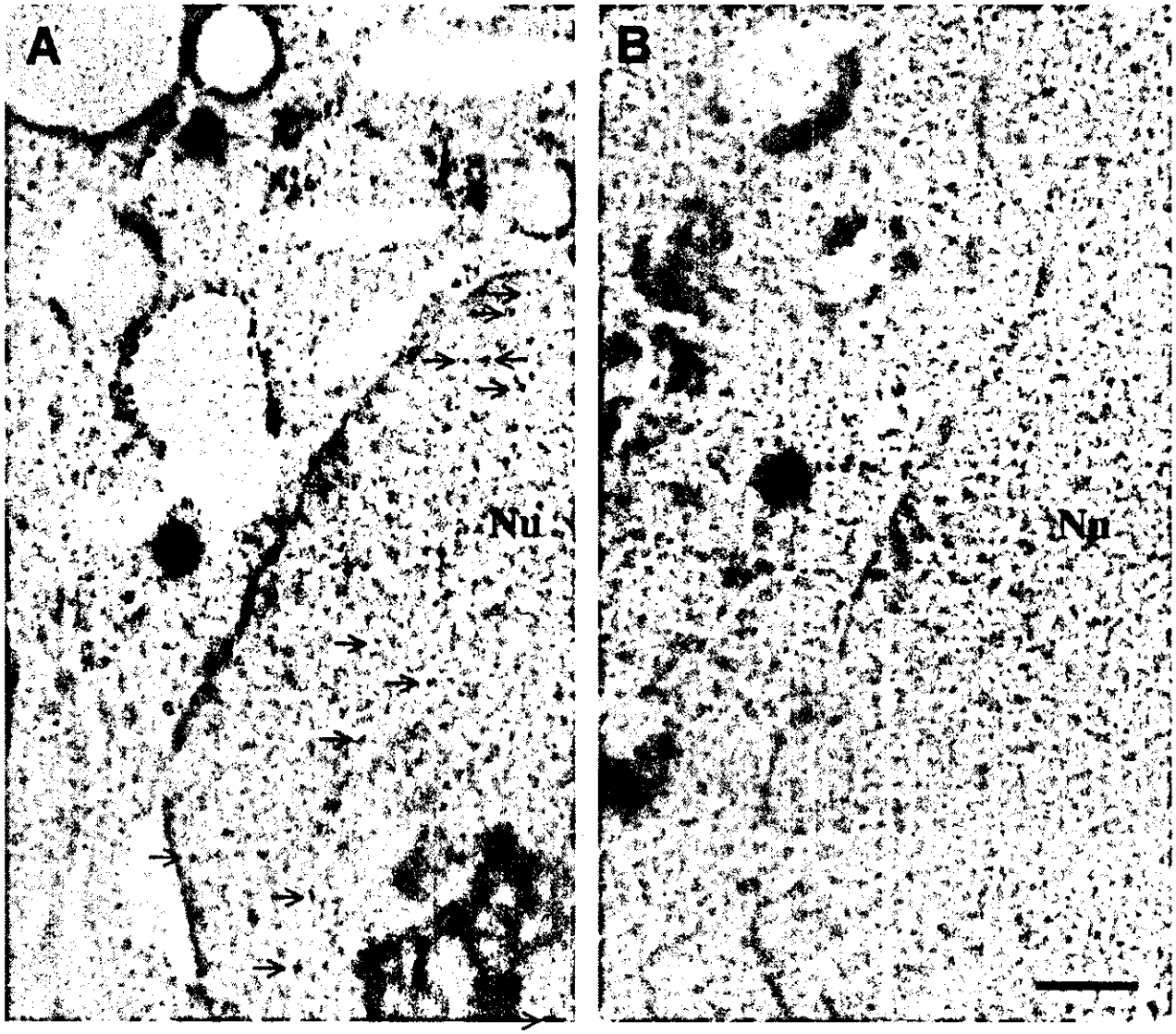

FIG. 3. Immunoelectron microscopy of HCV core protein. 293T cells expressing the full-length core protein (A) and nonexpressing cells (B) fixed 2 days after transfection. Immunoelectron microscopic analysis was performed with a mouse anticore antibody and a secondary anti-mouse IgG conjugated with gold particles. The arrows indicate the core protein localized in the nucleus (Nu). Bar, 500 nm.

calregulin, and a merged image, respectively). The pattern of subcellular localization of the core protein (Fig. 1d) was compared to the distribution of mitochondria, as revealed by MitoTracker staining (Fig. 1e). Although distribution of the core protein was not completely identical with that of the mitochondrion-selective dye, overlapping staining was observed, particularly in the perinuclear region (Fig. 1f).

Intracellular localization of the core protein was further examined in 293T cells by subcellular fractionation and Western blotting. The core protein was present in both the ER and mitochondrial fractions (Fig. 2), while it was not detected in the cytosol fraction (data not shown). The purity of the ER and mitochondrial fractions was confirmed with antibodies against ribophorin I as an ER marker and prohibitin as a mitochondrial marker.

It is generally difficult to identify the nuclear distribution of proteins of interest due to contamination of the nuclear preparation with unbroken, intact cells. Thus, to investigate whether the core protein localizes to the nucleus, we examined transfected cells by immunoelectron microscopy. Although gold particles were primarily observed within cytoplasmic membranes, perhaps highlighting the ER, immunoreactivity to anticore antibody was also observed in the nucleus (Fig. 3A, arrows). In contrast, no antibody labeling was observed in cells transfected with an empty vector (Fig. 3B).

Thus, HCV core protein predominates in the cytoplasm in a membrane-associated form(s) with ER and mitochondria, but nuclear localization is also observed.

Regions responsible for directing core protein to the ER and mitochondria. Given the tendency of the core protein to lo-

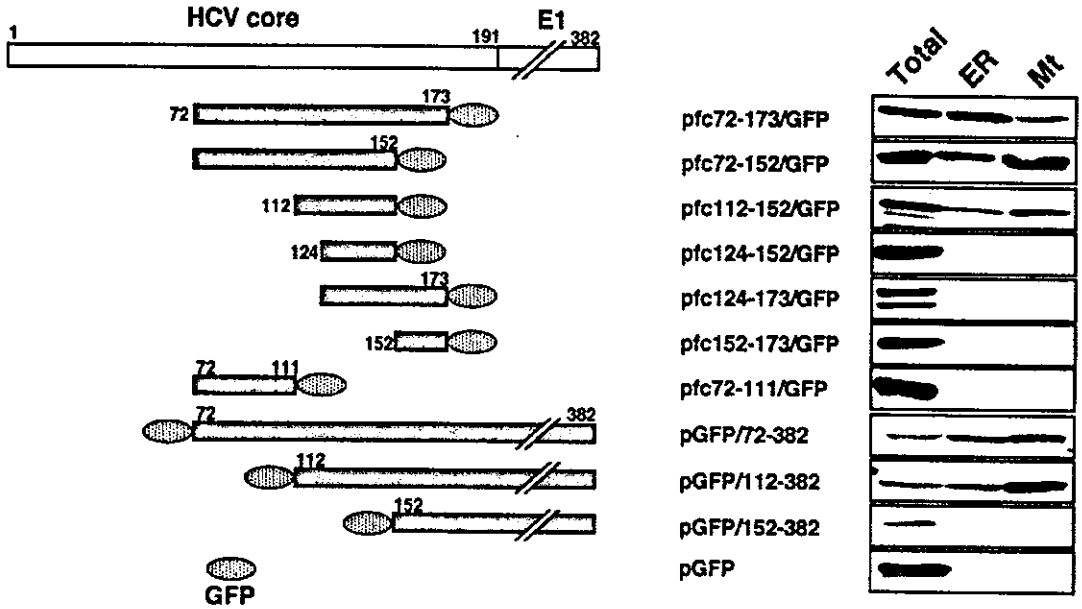

FIG. 4. Identification of segments that mediate association with ER and mitochondria in the core protein. Schematic diagram (left) and nomenclature (middle) of the core-GFP fusions are shown. Gray bars, expressed core and E1 regions. Subcellular distribution of fusion proteins is indicated on the right. ER and mitochondrial (Mt) fractions as well as whole-cell lysates (Total) were subjected to immunoblotting with an anti-GFP antibody.

calize to the ER and to mitochondria, we next investigated whether specific sequences might be responsible for transporting the core protein to these organelles. Fusion proteins between different regions of the core protein and GFP were developed, with specific emphasis on the region downstream of amino acid 72 because this region contains clusters of hydrophobic amino acids and the N-terminal 71 residues of the core are known to play a role in nuclear targeting (6, 48).

Western blotting of subcellular fractions with anti-GFP antibody revealed the localization of a core (72–173)-GFP fusion protein to the ER and to mitochondria (Fig. 4). Fusion proteins containing GFP and core proteins with N- or C-terminal deletions (72-152-GFP and 112-152-GFP) were likewise identified within the ER and mitochondrial fractions. In contrast, the ER and mitochondrial fractions did not contain GFP fusion proteins containing core protein amino acids 124 to 152, 124 to 173, 152 to 173, or 72 to 111. These fusion proteins demonstrated distribution profiles similar to that of GFP alone. We also tested GFP-core-E1 fusions, which are processed at the C terminus of the core by signal peptidase and signal peptide peptidase (19, 30). GFP-core fusions expressed from pGFP/72–382 and pGFP/112–382 were detected in the ER and mitochondrial fractions. The fusion expressed from pGFP/152–382 was not identified in these fractions.

We further analyzed subcellular localization of the fusion proteins by confocal immunofluorescence microscopy (Fig. 5). As expected, fusions of (72–173)-GFP and (112–152)-GFP exhibited localization to the ER and mitochondria. The patterns of subcellular localization of these fusions are indistinguishable from that of the full-length core protein, as shown in Fig. 1. Expression of (124–152)-GFP or (112–123)-GFP resulted in widespread diffusion of the fusion in the cell. Thus, these results indicate that the region spanning amino acids 112 to 152 can mediate association of the core protein not only to the ER but also to the mitochondria.

We subsequently examined the submitochondrial localization of the core protein with a protease protection assay. As shown in Fig. 6A, HCV core protein localized in the mitochondria was completely digested upon treatment with proteinase K for 30 min at 0°C. Under identical conditions, a marker specific for the mitochondrial outer membrane, Tom20, was also observed to disappear, whereas digestion of a mitochondrial inner membrane marker, Tim17, was not observed. These findings confirm that HCV core protein is localized to the mitochondrial outer membrane.

The predicted secondary structure of the region, amino acids 72 to 173, is shown in Fig. 6B. The presence of a long helical segment, lying between amino acids 116 and 134, and two short α-helices (amino acids 146 to 152 and amino acids 155 to 159) were predicted. The results of the cell fractionation assay and confocal microscopy with a series of deletion mutants shown in Fig. 4 and 5 suggest that an α-helix between amino acids 116 and 134 may be required for associating the core protein with the ER and the mitochondrial outer membrane. When amino acids 117 to 134 are portrayed as a helical wheel, we found an amphipathic structure with hydrophobic residues on one side and polar residues on the other side of the α-helix (Fig. 6C), which is often observed in membrane-associated proteins. This helical conformation might be important for directing the core protein to the ER and mitochondrial outer membranes.

Nuclear localization of the HCV core protein is mediated by a bipartite NLS, possibly via an importin-dependent pathway. Although HCV core protein is mainly localized within the cytoplasm, it is also found in the nucleus, as shown in Fig. 3.

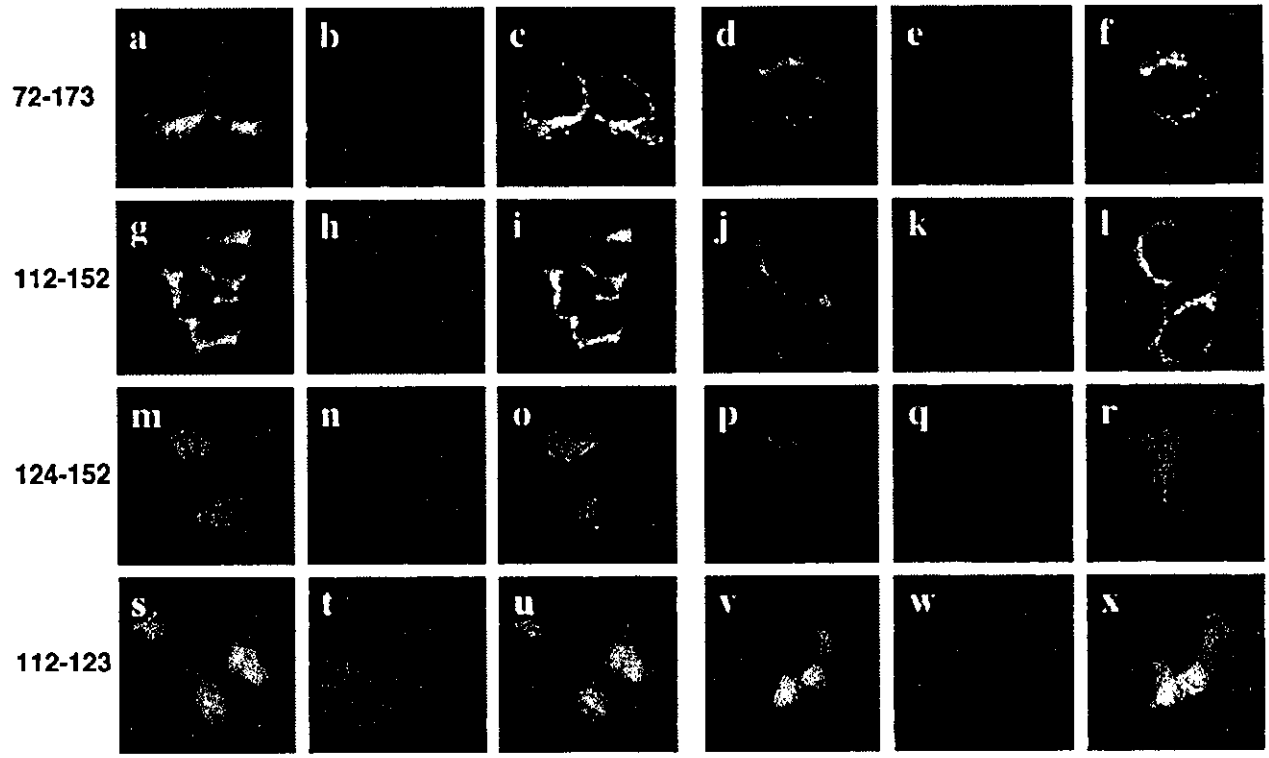

FIG. 5. Confocal analysis of double staining for core-GFP fusion protein and ER or mitochondria. 293T cells transfected with core-GFP expression plasmids (72–173, 112–152, 124–152, and 112–123) were allowed to express the plasmid for 2 days. Transfected cells were fixed directly (a to c, g to i, m to o, and s to u) or fixed after loading with Mitotracker (d to f, j to l, p to r, and v to x). After permeabilization with Triton X-100, a goat anticalregulin antibody was used for ER staining. The red signals corresponding to the ER were obtained with a rhodamine-conjugated rabbit anti-goat IgG secondary antibody (b, h, n, and t). Mitochondria were stained with the mitochondrion-selective dye Mitotracker (e, k, q, and w). Overlay resulted in yellow signals indicative of colocalization (c, f, i, l, o, r, u, and x).

The results of previous studies demonstrate that the N-terminal region of the core protein is responsible for nuclear targeting. It contains three clusters of basic amino acid residues that represent putative consensus motifs for NLS sequences PKPQRKTKR (amino acids 5 to 13), PRRGPR (amino acids 38 to 43), and PRGRRQPIPKARRP (amino acids 58 to 71) (6, 48). Nuclear targeting is generally governed by a family of transporters or cytosolic receptor proteins, known as importins or karyopherins, which function in concert with a guanine nucleotide-binding protein named Ran and other regulatory proteins such as NTF2/p10. Conventional NLS-dependent nuclear targeting occurs when importin-α recognizes the NLS sequence, mediating binding to importin-β1, after which the trimeric complex translocates to the nucleus (12).

In order to determine whether the putative NLS motifs identified within the core protein sequence are capable of binding to importin-α, we examined the in vitro interaction between bacterially expressed GST-fused core protein and ^{35}S-labeled importin-α with a GST pulldown assay. We then substituted lysine and arginine residues of one or more of the putative NLS motifs of the core protein (all contained within the first 71 amino acids of the N terminus) with alanine and fused the resultant constructs with GST, as shown schematically in Fig. 7A. As shown in Fig. 7B (upper panel), importin-α was pulled down by a GST fusion protein containing wild-type core (amino acids 1 to 71) protein but not with GST alone, suggesting that direct binding occurs between the core protein and importin-α. Importin-α was also pulled down by GST-core fusion proteins containing substitutions in one or two NLS motifs (NLS/m1, NLS/m2, NLS/m3, NLS/m4, NLS/m5, and NLS/m6). However, importin-α was not pulled down by GST-core fusion proteins containing alanine substitutions in all three NLS motifs (NLS/m7). It should be noted that similar amounts of GST fusion proteins were used for each of the in vitro pulldown assays, followed by SDS-PAGE and Coomassie brilliant blue staining (Fig. 7B, lower panel). These results demonstrated that all three putative NLS motifs of the N-terminal region of the core protein can mediate binding to importin-α, which suggests that nuclear translocation of the core protein occurs via an importin-dependent pathway (12).

The interaction between the core and importin-α was further analyzed by a colocalization assay (Fig. 7C). The GFP fusion containing the wild-type core (amino acids 1 to 71) was well colocalized with HA-importin-α; distribution of the two proteins showed similar nuclear staining patterns, confirming the presence of a functional NLS sequence(s) within the core protein. In contrast, NLS/m4, with substitutions in two NLS motifs, was partly colocalized with HA-importin-α near or around the nuclear membrane, suggesting that NLS motif double mutants bind to importin-α but their binding efficiency is lower than that of wild-type core protein.

Finally, we examined the subcellular localization of core

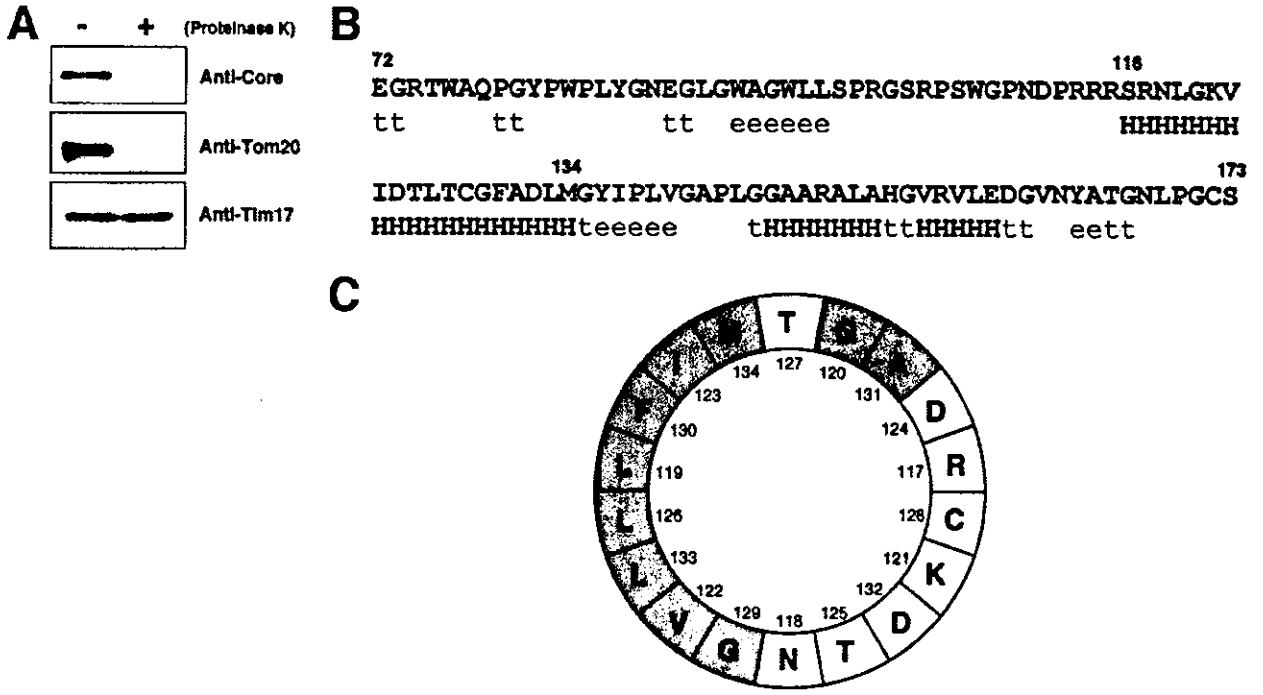

FIG. 6. (A) Protease protection assay. A mitochondrial fraction isolated from cells expressing the core protein was treated with proteinase K (+) as described in Materials and methods. The sample as well as the nontreated fraction (−) were subjected to immunoblotting with a monoclonal antibody against either HCV core, Tom20, or Tim17. (B) Protein sequence and predicted secondary structure of HCV core, amino acids 72 to 173. The secondary structure prediction was obtained with the self-optimized prediction method, a computer program on the internet (http://npsa-pbil.ibcp.fr/cgi-bin/npsa_automat.pl?page = /NPSA/npsa_sopm.html). H, α-helix; t, turn; e, extension. (C) α-Helical plot of amino acids 117 to 134 of the core protein. In the helical wheel plots, the gray shading represents apolar and hydrophobic residues; and the white represents polar residues.

protein expressed by the wild-type and NLS mutants (Fig. 7D). As expected, a fusion protein containing wild-type core protein (amino acids 1 to 71) and GFP was localized exclusively to the nucleus. Core proteins from three fusion proteins containing substitutions in each NLS motif (NLS/m1, NLS/m2, and NLS/m3) were detected primarily in the nucleus. Weak fluorescence was also observed in the cytoplasm, suggesting that these mutations caused a slight reduction in the efficiency of nuclear translocation. On the other hand, two or three NLS motif substitution mutations (NLS/m4, NLS/m5, NLS/m6, and NLS/m7) completely abolished nuclear translocation, resulting in a diffuse distribution of core protein, similar to that of GFP alone. Although it is likely that all three putative NLS motifs play a role, the above results suggest that at least two of the three putative NLS motifs are prerequisite for efficient nuclear translocation of the core protein.

DISCUSSION

HCV core protein is released from the viral polyprotein by a host protease(s) within the ER membrane at a signal peptide sequence lying between the core and envelope (E1) proteins (16, 41). Subsequently, the signal peptide is further processed by an intramembranous protease called signal peptide peptidase (38, 53). This mature form of the core protein is then released and undergoes subcellular trafficking (30, 53). The core protein localizes mainly to the ER, mitochondria, and lipid droplets. Some reports also describe localization of the core protein to the nuclei of hepatocytes in HCV-infected patients (10), transgenic mice (34), and cultured cells expressing viral polyproteins (56). Although it has been reported which sequence motifs are responsible for localization of the HCV core protein to lipid droplets and nuclei, it is uncertain which sequences target the core protein to the ER and to mitochondria. In this study, we identified sequences related to localization of the mature core protein to the ER and to mitochondria.

Through heterologous expression of core-GFP fusion proteins containing a series of deletions, we determined that a sequence extending from amino acids 112 to 152 of the core protein is required for its localization at the mitochondrial outer membrane. Translocation of nucleus-encoded mitochondrial proteins is usually dependent on N-terminal sequences, referred to as mitochondrial targeting sequences (37). However, it is also true that a significant proportion of mitochondrial proteins lack these N-terminal mitochondrial targeting sequences. Specifically, a number of outer membrane proteins do not have cleavable sequences at their N termini; rather, they are targeted to mitochondria by means of internal or C-terminal signals (31).

Since it has been reported that amino acid sequences required for targeting to the outer mitochondrial membrane form a highly hydrophobic α-helical wheel, as seen in A-kinase associated protein 84/12 (4) and NADH-cytochrome *b* reduc-